

Time-reversal symmetry breaking and unconventional superconductivity in Zr_3Ir : A new type of noncentrosymmetric superconductor

T. Shang,^{1,2,3,*} S. K. Ghosh,^{4,†} L. -J. Chang,⁵ C. Baines,⁶ M. K. Lee,⁵ J. Z. Zhao,⁷ J. A. T. Verezhak,⁶ D. J. Gawryluk,¹ E. Pomjakushina,¹ M. Shi,² M. Medarde,¹ J. Mesot,^{8,3,9} J. Quintanilla,⁴ and T. Shiroka^{9,8}

¹Laboratory for Multiscale Materials Experiments, Paul Scherrer Institut, Villigen CH-5232, Switzerland

²Swiss Light Source, Paul Scherrer Institut, Villigen CH-5232, Switzerland

³Institute of Condensed Matter Physics, École Polytechnique Fédérale de Lausanne (EPFL), Lausanne CH-1015, Switzerland.

⁴School of Physical Sciences, University of Kent, Canterbury CT2 7NH, United Kingdom

⁵Department of Physics, National Cheng Kung University, Tainan 70101, Taiwan

⁶Laboratory for Muon-Spin Spectroscopy, Paul Scherrer Institut, CH-5232 Villigen PSI, Switzerland

⁷Co-Innovation Center for New Energetic Materials, Southwest University of Science and Technology, Mianyang, 621010, People's Republic of China

⁸Paul Scherrer Institut, CH-5232 Villigen PSI, Switzerland

⁹Laboratorium für Festkörperphysik, ETH Zürich, CH-8093 Zurich, Switzerland

We report the discovery of a new type of unconventional noncentrosymmetric superconductor, Zr_3Ir with $T_c = 2.2$ K, investigated mostly via muon-spin rotation/relaxation (μSR) techniques. Its bulk superconductivity was characterized using magnetic susceptibility, electrical resistivity, and heat capacity measurements. The low-temperature superfluid density, determined via transverse-field μSR and electronic specific heat, suggests a fully-gapped superconducting state. The spontaneous magnetic fields, revealed by zero-field μSR below T_c , indicate the breaking of time-reversal symmetry in Zr_3Ir and, hence, the unconventional nature of its superconductivity. Our results suggest that Zr_3Ir belongs to a new class of materials, suitable for studying the interplay of gauge-, spatial-inversion-, and time-reversal symmetries.

Unconventional superconductors, in addition to the standard $U(1)$ gauge symmetry, break also other types of symmetry [1, 2]. Among them, the breaking of time-reversal symmetry (TRS) below T_c has been widely studied, in particular by means of zero-field muon-spin relaxation (ZF- μSR). This is a very sensitive technique, able to detect the tiny spontaneous magnetic fields appearing below the onset of superconductivity. Unconventional superconductors known to exhibit TRS breaking include Sr_2RuO_4 [3], PrOs_4Sb_4 [4], Upt_3 [5], LaNiGa_2 [6], LaNiC_2 , La_7T_3 , and ReT (T = transition metal) [7–14]. The latter three represent also typical examples of noncentrosymmetric superconductors (NCSCs), i.e., materials where besides TRS also the spatial-inversion symmetry is violated. In NCSC materials, the lack of inversion symmetry leads to an electric field gradient and, hence, to an antisymmetric spin-orbit coupling (ASOC), which splits the Fermi surface into spin-up and spin-down configurations. In most cases, the strength of ASOC exceeds the superconducting energy gap, and the pairing of electrons belonging to different spin-split bands results in a mixture of spin singlet- and triplet states. Due to such mixed pairing, NCSCs may exhibit significantly different properties compared to their conventional counterparts, e.g., a superconducting gap with nontrivial line- or point nodes [15–19] or upper critical fields exceeding the Pauli limit [9, 13, 20, 21].

In general, the breaking of time-reversal and spatial-inversion symmetries are not necessarily correlated, i.e., a lack of inversion symmetry does not imply a breaking of TRS. Indeed, many NCSC materials, such as $\text{Mo}_3\text{Al}_2\text{C}$ [22], LaTSi_3 [23–25], or $\text{Mg}_{10}\text{Ir}_{19}\text{B}_{16}$ [26], do not exhibit spontaneous magnetic fields and, hence, TRS is believed to be preserved in their superconducting state. On the other hand, enhanced electron-electron interactions and unconventional pairing mechanisms due to ASOC are considered to be the most likely causes of TRS breaking in NCSCs. For instance, the TRS breaking observed in LaNiC_2 [7, 27, 28] is proposed to originate from nonunitary triplet pairing. Gen-

erally, nonunitary refers to different pairing states for electrons belonging to spin-up and spin-down Fermi surfaces. In the particular case of nonunitary triplets, a nodeless multigap superconductivity is also expected. As for the role of electron-electron interactions, recent studies on La_7T_3 have shown that these might drive its nodeless superconductivity and justify the observed TRS-breaking state [8, 14].

Despite numerous examples of NCSCs, to date only a few of them are known to break also TRS in their superconducting state. The causes of such a selective TRS breaking remain largely unknown. Therefore, the availability of new NCSC compounds with a broken TRS, such as Zr_3Ir reported here, would help our understanding of the interplay between the different types of symmetry. Although the structure of the Zr_3Ir binary alloy is known since long time [29], its physical properties have never been studied. In this Letter, we report on systematic studies of Zr_3Ir by means of magnetization, transport, thermodynamic, and muon-spin relaxation (μSR) measurements. The key observation of spontaneous magnetic fields, revealed by zero-field (ZF) μSR , indicates that Zr_3Ir represents a new member of the NCSC class, that can serve as a testbench for current theories of TRS breaking and unconventional superconductivity in NCSCs.

Polycrystalline Zr_3Ir samples were prepared by arc melting Zr and Ir metals in a water-cooled copper hearth under high-purity argon atmosphere. The as-cast ingots were then annealed at 600°C over two weeks. The crystal structure and the sample purity were checked by means of room-temperature x-ray powder diffraction by using a Bruker D8 diffractometer. Zr_3Ir crystallizes in a tetragonal $\alpha\text{-V}_3\text{S}$ -type noncentrosymmetric structure with space group $I4_2m$ (121) [30]. The magnetic susceptibility, electrical resistivity, and specific heat measurements were performed on a 7-T Quantum Design Magnetic Property Measurement System equipped with a ^3He refrigerator and on a 14-T Physical Property Measurement System equipped with a dilution refrigerator (DR). The μSR measurements were carried out

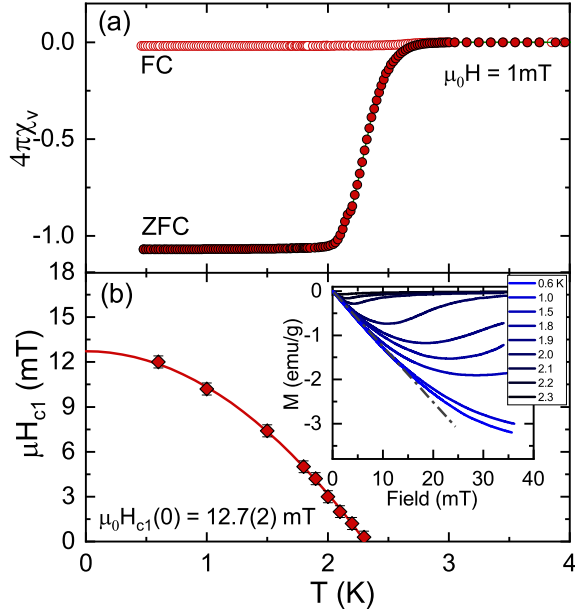


FIG. 1. (a) Temperature dependence of the zero-field cooled (ZFC) and field-cooled (FC) Zr_3Ir magnetic susceptibility, measured in an applied field of 1 mT. (b) Estimated $\mu_0 H_{c1}$ values vs. temperature; the solid line represents a fit to $\mu_0 H_{c1}(T) = \mu_0 H_{c1}(0)[1 - (T/T_c)^2]$. The inset shows the field-dependent magnetization $M(H)$ recorded at various temperatures (from 0.6 K to T_c). $\mu_0 H_{c1}$ was determined as the value where $M(H)$ deviates from linearity (dashed-dotted line).

on the GPS and LTF spectrometers of the $\pi\text{M}3$ beam line at the Paul Scherrer Institut (PSI), Villigen, Switzerland.

The temperature dependence of the magnetic susceptibility was studied using both FC- and ZFC- protocols in an applied field of 1 mT. The splitting of the two curves, shown in Fig. 1(a), is typical of type-II superconductors. The ZFC susceptibility indicates the onset superconductivity at 2.7 K, consistent with electrical resistivity data [30]. To determine $\mu_0 H_{c1}$, the field-dependent magnetization $M(H)$ was measured at various temperatures from 0.6 K up to T_c , as shown in the inset of Fig. 1(b). The estimated $\mu_0 H_{c1}$ values vs. temperature are plotted in Fig. 1(b). The solid line is a fit to $\mu_0 H_{c1}(T) = \mu_0 H_{c1}(0)[1 - (T/T_c)^2]$, which provides a lower critical field of 12.7(1) mT and a bulk T_c of 2.3 K, respectively. The bulk superconductivity of Zr_3Ir was further confirmed by specific-heat measurements [30].

To explore the nature of Zr_3Ir superconductivity at a microscopic level, we resort to transverse field (TF) μSR measurements. Here, a FC-protocol is used to induce a flux-line lattice (FLL) in the mixed superconducting state, successively probed via TF- μSR . The optimal field value for such experiments was determined via preliminary field-dependent μSR measurements at 1.5 K [30]. Figure 2(a) shows typical TF- μSR spectra, collected above and below T_c in an applied field of 30 mT. The time dependence of muon-spin asymmetry is described by:

$$A_{\text{TF}} = A_s e^{-\sigma^2 t^2/2} \cos(\gamma_\mu B_s t + \phi) + A_{\text{bg}} \cos(\gamma_\mu B_{\text{bg}} t + \phi). \quad (1)$$

Here A_s and A_{bg} are the sample and background asymmetries, with the latter not undergoing any depolarization. $\gamma_\mu/2\pi = 135.53 \text{ MHz/T}$ is the muon gyromagnetic ratio, B_s and B_{bg} are the local fields sensed by implanted muons

in the sample and the sample holder, ϕ is a shared initial phase, and σ is a Gaussian relaxation rate, related to the field-distribution inside the sample. The large σ below T_c reflects the inhomogeneous field distribution due to the FLL. In the superconducting state, the Gaussian relaxation rate includes contributions from both the FLL (σ_{FLL}) and a smaller, temperature-independent relaxation, due to nuclear moments (σ_n). The FLL-related relaxation can be ex-

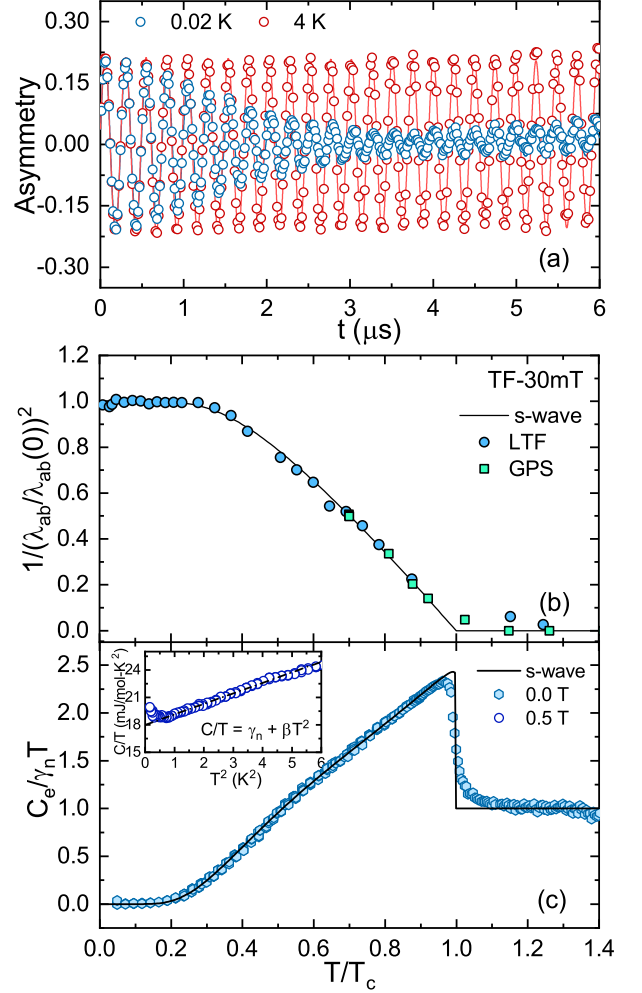


FIG. 2. (a) Time-domain TF- μSR spectra in the superconducting (0.02 K) and the normal (4 K) phase of Zr_3Ir . The normalized superfluid density (b) and zero-field electronic specific heat (c) vs. the reduced temperature (T/T_c). The inset in (c) shows the raw C/T data measured in a 0.5-T applied field as a function of T^2 . The dashed-line is a fit to $C/T = \gamma_n + \beta T^2$, from which the phonon contribution was evaluated. The solid lines in (b) and (c) represent fits using a fully-gapped s-wave model.

tracted by subtracting the nuclear contribution in quadrature, i.e., $\sigma_{\text{FLL}} = \sqrt{\sigma^2 - \sigma_n^2}$. Since σ_{FLL} is directly related to the magnetic penetration depth and the superfluid density ($\sigma_{\text{FLL}} \propto 1/\lambda^2$), the superconducting gap value and its symmetry can be determined from the measured relaxation rate.

Since the upper critical field μH_{c2} of Zr_3Ir is relatively modest (0.62 T) [30], to extract the effective penetration depth λ_{eff} from the measured σ_{FLL} we had to use the expression [31, 32]

$$\sigma_{\text{FLL}}(h) = 0.172 \frac{\gamma_\mu \Phi_0}{2\pi} (1-h) [1 + 1.21(1 - \sqrt{h})^3] \lambda_{\text{eff}}^{-2}, \quad (2)$$

valid for intermediate values of the reduced magnetic field, $h = H_{\text{appl}}/H_{c2}$, with $H_{\text{appl}} = 30$ mT in our case. In a polycrystalline sample, the effective penetration depth λ_{eff} is usually determined by the shortest penetration depth λ_{ab} , the two being related via $\lambda_{\text{eff}} = 3^{1/4}\lambda_{ab}$ [33]. Figure 2(b) shows the normalized superfluid density ($\rho_{\text{sc}} \propto 1/\lambda_{ab}^2$) versus the reduced temperature T/T_c for Zr_3Ir . The data collected on GPS and LTF spectrometers are highly consistent. For $T < 0.3 T_c$, the superfluid density is nearly temperature independent, indicating the absence of energy excitations and, hence, a fully-gapped superconductivity. The temperature-dependent superfluid density was further analyzed by an s -wave model with a single superconducting gap, which provides $\Delta(0) = 0.30(1)$ meV and $\lambda_{ab}(0) = 221(2)$ nm. Such gap value yields $2\Delta/k_B T_c = 3.24(4)$, comparable with the BCS value of 3.53. This indicates a weak electron-phonon coupling in Zr_3Ir , consistent with the electron-phonon coupling constant estimated from specific-heat measurements [30].

The zero-field specific-heat data were further analyzed to get more insight into the superconducting properties. After subtracting the phonon contribution (βT^2 -term) from the experimental data, the derived electronic specific heat C_e/T divided by γ_n is presented in Fig. 2(c) versus the reduced temperature T/T_c . The solid-line through the zero-field data represents a fit with $\gamma_n = 19 \text{ mJ mol}^{-1} \text{K}^{-2}$ and a single isotropic gap, $\Delta(0) = 0.32(1)$ meV. Both zero-field specific-heat and TF- μSR results are thus fully compatible with an s -wave superconductivity model. Finally, the specific-heat jump at T_c was found to be $\Delta C/\gamma T_c \sim 1.32$, i.e., comparable with the BCS value of 1.43, again indicating a weak electron-phonon coupling in Zr_3Ir .

ZF- μSR measurements were used to establish the onset of TRS breaking in the superconducting phase through its key signature, the appearance of spontaneous magnetic fields below T_c . The large muon gyromagnetic ratio, combined with the availability of 100% spin-polarized muon beams, make ZF- μSR a very suitable technique to detect weak spontaneous fields, down to ~ 0.01 mT [34]. In the absence of external fields, the ZF muon-spin relaxation rate is not expected to change while entering the superconducting phase. However, in case of broken TRS, the accompanying onset of spontaneous currents gives rise to weak internal fields, causing an increase in the ZF muon-spin relaxation rate. Given the tiny size of such effects, one should compare the ZF relaxation rates above T_c with those deep inside the superconducting phase. Representative ZF- μSR spectra, shown in Fig. 3(a), indicate a clear change in the muon-spin relaxation between 3 K and 0.02 K. Also, no visible muon precession could be detected, hence ruling out any magnetically ordered phases. For nonmagnetic materials, in the absence of applied fields, the depolarization of muon spins is mainly determined by the randomly oriented nuclear moments. This behavior is normally described by a Gaussian Kubo-Toyabe relaxation function [35, 36], as in the case of Re-based NCSC [9–13]. However, in the Zr_3Ir case, the depolarization is more consistent with a Lorentzian decay function. The attempts of using combined Gaussian and Lorentzian Kubo-Toyabe function as used in Ref. 9 lead zero value of Gaussian decay. This suggests that the fields sensed by the implanted muons arise from diluted nuclear

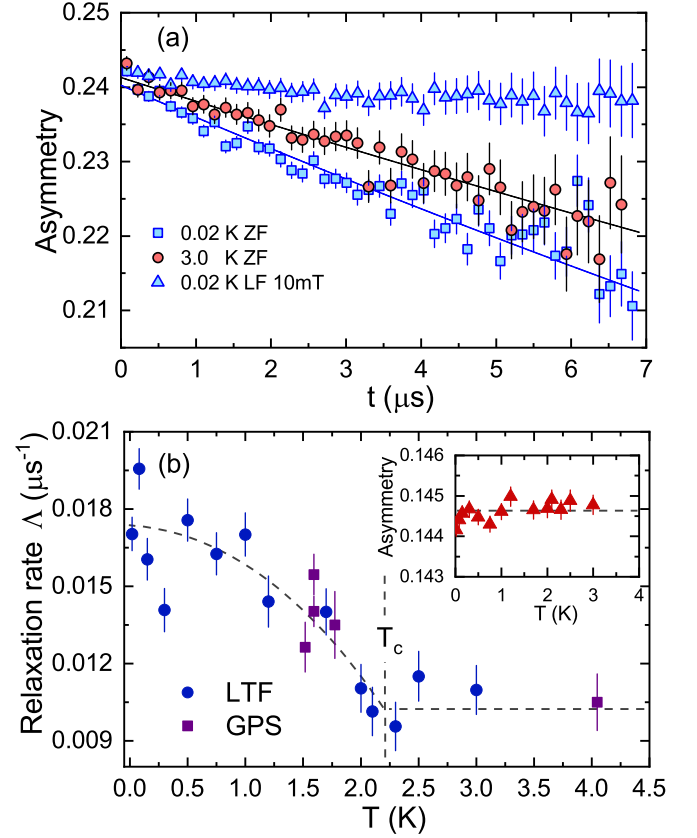


FIG. 3. Representative zero-field μSR spectra in the superconducting (0.02 K) and the normal (3 K) phase of Zr_3Ir , together with longitudinal field data (triangles), collected at 0.02 K and 10 mT. The solid lines are fits using a Lorentzian-decay function [see Eq. (3)]. (b) Derived relaxation rate Λ vs. temperature. The inset shows the evolution of asymmetry with temperature. The dashed lines are guides to the eye. The background signal was determined by comparing the data sets collected on the GPS and LTF spectrometers at the same temperature.

moments. The solid lines in Fig. 3(a) are fits to a simple Lorentzian function:

$$A_{\text{ZF}} = A_s \left\{ \frac{1}{3} + \frac{2}{3} (1 - \Lambda t) e^{-\Lambda t} \right\} + A_{\text{bg}}. \quad (3)$$

Here A_s and A_{bg} are the same as in the TF- μSR case. The 2/3-relaxing and 1/3-nonrelaxing components of the asymmetry originate from the powder average of the internal fields with respect to the initial muon-spin orientation in polycrystalline samples. The derived muon-spin relaxation rate Λ vs. temperature is summarized in Fig. 3(b). The relative change of the relaxation rate in Zr_3Ir is comparable to that in other NCSCs [7–14], with $\Lambda(T)$ showing a distinct increase below the onset of superconductivity, while being almost temperature independent above T_c . Such increase of $\Lambda(T)$ below T_c was also found in other compounds, e.g., La_7Ir_3 , LaNiC_2 , and SrRuO_3 [3, 7, 8], where it reflects the onset of spontaneous magnetic fields. This provides unambiguous evidence that TRS is also broken in the superconducting state of Zr_3Ir .

Note that the small magnitude of $\Lambda(T)$ in the Zr_3Ir case is due to its small nuclear magnetic moments. As a comparison, in La_7Ir_3 [8], the average nuclear moment is around $2.32 \mu_N$, twice larger than $1.13 \mu_N$ of Zr_3Ir , hence implying a Λ value which is also twice larger in the La_7Ir_3 case. To

rule out the possibility of extrinsic effects related to a defect/impurity induced relaxation at low temperatures, we also carried out auxiliary longitudinal-field μ SR measurements at base temperature (0.02 K). As shown in Fig. 3(a), a small field of 10 mT is sufficient to lock the muon spins and, hence, to fully decouple them from the weak spontaneous magnetic fields. This further supports the intrinsic nature of TRS breaking in the superconducting state of Zr_3Ir .

To date, the TRS breaking has been shown to occur in three structurally different NCSCs. These include the CeNiC_2 -type LaNiC_2 [7], the α -Mn-type ReT [9–13], and the Th_7Fe_3 -type La_7T_3 [8, 14]. With the α - V_3S -type Zr_3Ir reported here we bring evidence of a new NCSC class with broken TRS, structurally different from the known ones. However, it should be clear that, while structure might influence the occurrence of TRS breaking in NCSCs, its role is not well known. Thus, not only many NCSCs, e.g., $\text{Mo}_3\text{Al}_2\text{C}$, LaTSi_3 , $\text{Mg}_{10}\text{Ir}_{19}\text{B}_{16}$, and Re_3W [22–26, 37] preserve TRS, but the later two share the same α -Mn-type structure with other TRS-breaking ReT NCSCs. Moreover, the pairing mechanism in NCSC with preserved TRS seems to be dominated by the spin-singlet channel. On the other hand, in some of these NCSC, the changes in muon-spin relaxation between the normal and superconducting states are below the resolution of the μ SR technique (0.01 mT).

We discuss now the origin of TRS in unconventional superconductors. In general, a broken TRS does not necessarily imply triplet pairing only. Depending on the pairing mechanisms at play, two possible causes might be at the base of the observed spontaneous fields in the superconducting state. If Cooper pairs have both nonzero spin- and orbital moments, the twice (or more) degenerate superconducting phases lead to a spatially inhomogeneous order parameter around impurities, surfaces, or domain walls, in turn creating undamped spontaneous supercurrents in those regions [1, 4, 38]. A typical example of this possibility is given by Sr_2RuO_4 [3]. On the other hand, if Cooper pairs have only nonzero spin-moments, i.e., form nonunitary spin triplets, a hyperfine field is generated by the nonzero spin-moment at the muon stopping sites. Such case is typified by LaNiC_2 and LaNiGa_2 [6, 7, 28]. Similar to LaNiC_2 , Sr_2RuO_4 , and La_7T_3 , in Zr_3Ir , the spontaneous magnetic fields also appear in the Lorentzian relaxation channel. In contrast to multigapped LaNiC_2 or nodal Sr_2RuO_4 [3, 7], both La_7T_3 and Zr_3Ir exhibit nodeless superconductivity with a single gap, which can also break the TRS due to the highly-symmetric crystal structure [39]. Although a mixed pairing is allowed in both La_7T_3 and Zr_3Ir , due to the same-sign or near-equal magnitude of the order parameter in the two spin-split Fermi surfaces, the parity-mixing effects might be difficult to observe or hard to distinguish from those of conventional superconductors [40]. From the above, it seems that the nonunitary spin-triplet pairing is likely cause at the origin of broken TRS in Zr_3Ir . Yet, to unambiguously establish the nonunitary superconductivity of Zr_3Ir , further theoretical work — including group-theory analyses — is required.

In conclusion, we have discovered a new structurally different member of the NCSC class, Zr_3Ir , and investigate it by means of magnetization, transport, thermodynamic, and μ SR measurements. Both the zero-field specific-heat data

and superfluid density (from TF- μ SR) reveal a nodeless superconductivity below $T_c = 2.2(1)$ K, well described by an isotropic s -wave model with a single gap. The spontaneous magnetic fields detected by ZF- μ SR, which appear below T_c and increase with decreasing temperature, provide solid evidence that the superconducting state of Zr_3Ir breaks the TRS and has an unconventional nature. Considering its different structure from the known NCSC, Zr_3Ir is expected to stimulate further studies on the interplay among the space-, time-, and gauge symmetries in establishing the peculiar properties of the NCSC materials.

This work was supported by the Schweizerische Nationalfonds zur Förderung der Wissenschaftlichen Forschung (SNF) (Grants No. 20021-169455 and No. 206021-139082) S. K. G. and J. Q. are supported by EPSRC through the project “Unconventional Superconductors: New paradigms for new materials” (Grant No. EP/P00749X/1). L. J. C thanks the MOST funding supports under the projects 104-2112-M-006-010-MY3 and 107-2112-M-006-020 We also acknowledge the assistance from $S\mu$ S beamline scientists at PSI.

* Corresponding authors:

tian.shang@psi.ch

† Corresponding authors:

S.Ghosh@kent.ac.uk

- [1] M. Sigrist and K. Ueda, “Phenomenological theory of unconventional superconductivity,” *Rev. Mod. Phys.* **63**, 239–311 (1991).
- [2] C. C. Tsuei and J. R. Kirtley, “Pairing symmetry in cuprate superconductors,” *Rev. Mod. Phys.* **72**, 969–1016 (2000).
- [3] G. M. Luke, Y. Fudamoto, K. M. Kojima, M. I. Larkin, J. Merrin, B. Nachumi, Y. J. Uemura, Y. Maeno, Z. Q. Mao, Y. Mori, H. Nakamura, and M. Sigrist, “Time-reversal symmetry-breaking superconductivity in Sr_2RuO_4 ,” *Nature* **394**, 558 (1998).
- [4] Y. Aoki, A. Tsuchiya, T. Kanayama, S. R. Saha, H. Sugawara, H. Sato, W. Higemoto, A. Koda, K. Ohishi, K. Nishiyama, and R. Kadono, “Time-reversal symmetry-breaking superconductivity in heavy-fermion $\text{PrOs}_4\text{Sb}_{12}$ detected by muon-spin relaxation,” *Phys. Rev. Lett.* **91**, 067003 (2003).
- [5] G. M. Luke, A. Keren, L. P. Le, W. D. Wu, Y. J. Uemura, D. A. Bonn, L. Taillefer, and J. D. Garrett, “Muon spin relaxation in UPt_3 ,” *Phys. Rev. Lett.* **71**, 1466–1469 (1993).
- [6] A. D. Hillier, J. Quintanilla, B. Mazidian, J. F. Annett, and R. Cywinski, “Nonunitary triplet pairing in the centrosymmetric superconductor LaNiGa_2 ,” *Phys. Rev. Lett.* **109**, 097001 (2012).
- [7] A. D. Hillier, J. Quintanilla, and R. Cywinski, “Evidence for time-reversal symmetry breaking in the noncentrosymmetric superconductor LaNiC_2 ,” *Phys. Rev. Lett.* **102**, 117007 (2009).
- [8] J. A. T. Barker, D. Singh, A. Thamizhavel, A. D. Hillier, M. R. Lees, G. Balakrishnan, D. McK. Paul, and R. P. Singh, “Unconventional superconductivity in La_7Ir_3 revealed by muon spin relaxation: Introducing a new family of noncentrosymmetric superconductor that breaks time-reversal symmetry,” *Phys. Rev. Lett.* **115**, 267001 (2015).
- [9] T. Shang, G. M. Pang, C. Baines, W. B. Jiang, W. Xie, A. Wang, M. Medarde, E. Pomjakushina, M. Shi, J. Mesot, H. Q. Yuan, and T. Shiroka, “Nodeless superconductivity and time-reversal symmetry breaking in the noncentrosymmetric superconductor Re_{24}Ti ,” *Phys. Rev. B* **97**, 020502 (2018).
- [10] T. Shang, M. Smidman, S. K. Ghosh, C. Baines, L. J. Chang,

- D. J. Gawryluk, J. A. T. Barker, R. P. Singh, D. McK. Paul, G. Balakrishnan, E. Pomjakushina, M. Shi, M. Medarde, A. D. Hillier, H. Q. Yuan, J. Quintanilla, J. Mesot, and T. Shiroka, "Time-reversal symmetry breaking in re-based superconductors," *Phys. Rev. Lett.* **121**, 257002 (2018).
- [11] R. P. Singh, A. D. Hillier, B. Mazidian, J. Quintanilla, J. F. Annett, D. McK. Paul, G. Balakrishnan, and M. R. Lees, "Detection of time-reversal symmetry breaking in the non-centrosymmetric superconductor Re_6Zr using muon-spin spectroscopy," *Phys. Rev. Lett.* **112**, 107002 (2014).
- [12] D. Singh, J. A. T. Barker, A. Thamizhavel, D. McK. Paul, A. D. Hillier, and R. P. Singh, "Time-reversal symmetry breaking in the noncentrosymmetric superconductor Re_6Hf : Further evidence for unconventional behavior in the α -Mn family of materials," *Phys. Rev. B* **96**, 180501 (2017).
- [13] D. Singh, Sajilesh K. P., J. A. T. Barker, D. McK. Paul, A. D. Hillier, and R. P. Singh, "Time-reversal symmetry breaking in the noncentrosymmetric superconductor Re_6Ti ," *Phys. Rev. B* **97**, 100505 (2018).
- [14] D. Singh, M. S. Scheurer, A. D. Hillier, and R. P. Singh, "Time-reversal-symmetry breaking and unconventional pairing in the noncentrosymmetric superconductor La_7Rh_3 probed by μSR ," (2018), [arXiv:1802.01533 \[cond-mat\]](https://arxiv.org/abs/1802.01533).
- [15] H. Q. Yuan, D. F. Agterberg, N. Hayashi, P. Badica, D. Vandervelde, K. Togano, M. Sigrist, and M. B. Salamon, "s-wave spin-triplet order in superconductors without inversion symmetry: $\text{Li}_2\text{Pd}_3\text{B}$ and $\text{Li}_2\text{Pt}_3\text{B}$," *Phys. Rev. Lett.* **97**, 017006 (2006).
- [16] M. Nishiyama, Y. Inada, and Guo-qing Zheng, "Spin triplet superconducting state due to broken inversion symmetry in $\text{Li}_2\text{Pt}_3\text{B}$," *Phys. Rev. Lett.* **98**, 047002 (2007).
- [17] I. Bonalde, W. Brämer-Escamilla, and E. Bauer, "Evidence for line nodes in the superconducting energy gap of non-centrosymmetric CePt_3Si from magnetic penetration depth measurements," *Phys. Rev. Lett.* **94**, 207002 (2005).
- [18] G. M. Pang, M. Smidman, W. B. Jiang, J. K. Bao, Z. F. Weng, Y. F. Wang, L. Jiao, J. L. Zhang, G. H. Cao, and H. Q. Yuan, "Evidence for nodal superconductivity in quasi-one-dimensional $\text{K}_2\text{Cr}_3\text{As}_3$," *Phys. Rev. B* **91**, 220502 (2015).
- [19] D. T. Adroja, A. Bhattacharyya, M. Telling, Yu. Feng, M. Smidman, B. Pan, J. Zhao, A. D. Hillier, F. L. Pratt, and A. M. Strydom, "Superconducting ground state of quasi-one-dimensional $\text{K}_2\text{Cr}_3\text{As}_3$ investigated using μSR measurements," *Phys. Rev. B* **92**, 134505 (2015).
- [20] E. Bauer, G. Hilscher, H. Michor, C. Paul, E. W. Scheidt, A. Gribov, Y. Seropegin, H. Noël, M. Sigrist, and P. Rogl, "Heavy fermion superconductivity and magnetic order in noncentrosymmetric CePt_3Si ," *Phys. Rev. Lett.* **92**, 027003 (2004).
- [21] E. M. Carnicom, W. W. Xie, T. Klimczuk, J. J. Lin, K. Górnica, Z. Sobczak, N. P. Ong, and R. J. Cava, " TaRh_2B_2 and NbRh_2B_2 : Superconductors with a chiral noncentrosymmetric crystal structure," *Sci. Adv.* **4**, 7969 (2018).
- [22] E. Bauer, G. Rogl, Xing-Qiu Chen, R. T. Khan, H. Michor, G. Hilscher, E. Royanian, K. Kumagai, D. Z. Li, Y. Y. Li, R. Podloucky, and P. Rogl, "Unconventional superconducting phase in the weakly correlated noncentrosymmetric $\text{Mo}_3\text{Al}_2\text{C}$ compound," *Phys. Rev. B* **82**, 064511 (2010).
- [23] V. K. Anand, A. D. Hillier, D. T. Adroja, A. M. Strydom, H. Michor, K. A. McEwen, and B. D. Rainford, "Specific heat and μSR study on the noncentrosymmetric superconductor LaRhSi_3 ," *Phys. Rev. B* **83**, 064522 (2011).
- [24] V. K. Anand, D. Britz, A. Bhattacharyya, D. T. Adroja, A. D. Hillier, A. M. Strydom, W. Kockelmann, B. D. Rainford, and K. A. McEwen, "Physical properties of non-centrosymmetric superconductor LaIrSi_3 : A μSR study," *Phys. Rev. B* **90**, 014513 (2014).
- [25] M. Smidman, A. D. Hillier, D. T. Adroja, M. R. Lees, V. K. Anand, R. P. Singh, R. I. Smith, D. M. Paul, and G. Balakrishnan, "Investigations of the superconducting states of noncentrosymmetric LaPdSi_3 and LaPtSi_3 ," *Phys. Rev. B* **89**, 094509 (2014).
- [26] A. A. Aczel, T. J. Williams, T. Goko, J. P. Carlo, W. Yu, Y. J. Uemura, T. Klimczuk, J. D. Thompson, R. J. Cava, and G. M. Luke, "Muon spin rotation/relaxation measurements of the noncentrosymmetric superconductor $\text{Mg}_{10}\text{Ir}_{19}\text{B}_{16}$," *Phys. Rev. B* **82**, 024520 (2010).
- [27] J. Quintanilla, A. D. Hillier, J. F. Annett, and R. Cywinski, "Relativistic analysis of the pairing symmetry of the noncentrosymmetric superconductor LaNiC_2 ," *Phys. Rev. B* **82**, 174511 (2010).
- [28] Z. F. Weng, J. L. Zhang, M. Smidman, T. Shang, J. Quintanilla, J. F. Annett, M. Nicklas, G. M. Pang, L. Jiao, W. B. Jiang, Y. Chen, F. Steglich, and H. Q. Yuan, "Two-gap superconductivity in LaNiGa_2 with nonunitary triplet pairing and even parity gap symmetry," *Phys. Rev. Lett.* **117**, 027001 (2016).
- [29] K. Cenizual and E. Parthié, " Zr_3Ir with tetragonal α - V_3S structure," *Acta Cryst. C* **41**, 820 (1985).
- [30] See the Supplementary Material for details on the measurements of crystal structure, electrical resistivity, heat capacity, and critical field, as well as for the data analysis, and DFT calculation.
- [31] W. Barford and J. M. F. Gunn, "The theory of the measurement of the London penetration depth in uniaxial type II superconductors by muon spin rotation," *Physica C* **156**, 515 (1988).
- [32] E. H. Brandt, "Properties of the ideal Ginzburg-Landau vortex lattice," *Phys. Rev. B* **68**, 054506 (2003).
- [33] V. I. Fesenko, V. N. Gorbunov, and V. P. Smilga, "Analytical properties of muon polarization spectra in type-II superconductors and experimental data interpretation for mono- and polycrystalline HTSCs," *Physica C* **176**, 551 (1991).
- [34] A. Amato, "Heavy-fermion systems studied by μSR technique," *Rev. Mod. Phys.* **69**, 1119–1180 (1997).
- [35] R. Kubo and T. Toyabe, *Magnetic Resonance and Relaxation*, edited by R. Blinc (North-Holland, Amsterdam, 1967).
- [36] A. Yaouanc and P. Dalmas de Réotier, *Muon Spin Rotation, Relaxation, and Resonance: Applications to Condensed Matter* (Oxford University Press, Oxford, 2011).
- [37] P. K. Biswas, A. D. Hillier, M. R. Lees, and D. McK. Paul, "Comparative study of the centrosymmetric and non-centrosymmetric superconducting phases of Re_3W using muon spin spectroscopy and heat capacity measurements," *Phys. Rev. B* **85**, 134505 (2012).
- [38] C. H. Choi and P. Muzikar, "Impurity-induced magnetic fields in unconventional superconductors," *Phys. Rev. B* **39**, 9664–9666 (1989).
- [39] D. F. Agterberg, V. Barzykin, and Lev P. Gor'kov, "Conventional mechanisms for exotic superconductivity," *Phys. Rev. B* **60**, 14868 (1999).
- [40] S. Yip, "Noncentrosymmetric superconductors," *Annu. Rev. Condens. Matter Phys.* **5**, 15 (2014).